Bioorganic Chemistry 93 (2019) 103256

Contents lists available at ScienceDirect

Bioorganic Chemistry

journal homepage: www.elsevier.com/locate/bioorg

Anti-inflammatory evaluation and structure-activity relationships of diterpenoids isolated from *Euphorbia hylonoma*

Wen-Jun Wei[a], Weiyan Qi[b], Xin-Mei Gao[b], Ke-Na Feng[c], Kai-Liang Ma[a], Hang-Ying Li[a], Ya Li[a,*], Kun Gao[a,*]

[a] State Key Laboratory of Applied Organic Chemistry, College of Chemistry and Chemical Engineering, Lanzhou University, Lanzhou 730000, People's Republic of China
[b] Department of Marine Pharmacy, School of Life Science and Technology, China Pharmaceutical University, Nanjing 211198, People's Republic of China
[c] State Key Laboratory of Phytochemistry and Plant Resources in West China, and Yunnan Key Laboratory of Natural Medicinal Chemistry, Kunming Institute of Botany, Chinese Academy of Sciences, Kunming 650201, People's Republic of China

ARTICLE INFO

Keywords:
Euphorbia hylonoma
ent-Isopimarane
ent-Rosane
Anti-inflammatory

ABSTRACT

A phytochemical investigation to obtain chemical components with potential anti-inflammatory activity from *E. hylonoma* led to the isolation of nine new *ent*-isopimarane diterpenoids (**1** and **3**–**10**), a new *ent*-rosane diterpenoid (**11**), along with eight known ones (**2** and **12**–**18**) using various chromatographic techniques. Compounds **3**, **4**, **5**, and **10** were rare examples of the epoxy-*ent*-isopimarane. The structures of these new compounds were confirmed by extensive spectroscopic data, crystal X-ray diffraction analysis, and electronic circular dichroism. And the isolates were evaluated for their inhibitory effects on nitric oxide production induced by lipopolysaccharide in RAW 264.7 cells. The results showed that compounds **2** and **12** exhibited noteworthy inhibitory effects against NO production with IC_{50} values of 7.12 and 12.73 μM, respectively, which were better than positive control (IC_{50} = 41.41 μM). The possible mechanism that compounds **2** and **12** could inhibit NO production was investigated by the Western blotting experiments.

1. Introduction

Nitric oxide (NO) is a well-known signaling molecule in cells, which plays a key role in many physiological processes. The pharmacological studies have demonstrated that the inflammation is related to the excessive production of NO. Thus, the inhibition of NO production may be an important target in the treatment of inflammatory diseases. Meanwhile, the level of NO has been used as an important marker for researching the mechanism of inflammation [1–3].

The genus *Euphorbia* belongs to Euphorbiaceae family, which is widely distributed throughout the world. This genus is one of the largest genera in the angiosperm plants, consisting of approximately 2000 species [4]. Many plants in this genus have been used as folk medicine in China to treat diarrhea, enteritis, dermatitis, gingival bleeding, and jaundice, which could be attributed to the existence of various bioactive secondary metabolites [5,6]. In recent years, the phytochemical research of the genus *Euphorbia* mainly led to the isolation of various diterpenoids, such as jatrophane, *ent*-isopimarane, tigliane, *ent*-atisane and *ent*-kaurane. Meanwhile, these diterpenoids showed a variety of biological activities, such as anti-inflammatory [7,8], antiadipogenic [9], phytotoxicity [10], antiviral [11], and P-glycoprotein inhibitory activity [12].

Euphorbia hylonoma, known as "Jiu Niuzao" in folk medicine in China, is used for treatment of liver cancer, hepatocirrhosis, edema, and incontinence [13]. But there are few reports regarding either the chemical compositions or the biological activities of *E. hylonoma*. In our work, the EtOAc fraction of the roots of *E. hylonoma* at 50 μg/ml was tested for its inhibitory effect on the NO production induced by lipopolysaccharide (LPS) in RAW 264.7 cells. And it exhibited significant inhibitory effect with inhibition rate of 78%, which inspired us to further explore the chemical components with anti-inflammatory activity from this plant. Therefore, the aim of this study is to search for and isolate natural products with anti-inflammatory activity.

Herein, a phytochemical investigation of the EtOAc fraction of the roots of *E. hylonoma* was carried out, producing 10 new and 8 known diterpenoids. In addition, we tested the NO inhibitory effects of the isolated compounds to search for potential lead compounds.

* Corresponding authors.
E-mail addresses: liea@lzu.edu.cn (Y. Li), npchem@lzu.edu.cn (K. Gao).

https://doi.org/10.1016/j.bioorg.2019.103256
Received 17 April 2019; Received in revised form 5 August 2019; Accepted 4 September 2019
Available online 17 September 2019

Table 1
^{1}H NMR data of compounds **1–5** in $CDCl_3$.

Position	δ_H (*J* in Hz)				
	1[b]	**3**[a]	**4**[a]	**5**[a]	**6**[c]
1a	1.36 dd (3.0, 14.4)	1.55 m overlapped	3.27 d (4.0)	3.14 d (3.6)	3.86 br s
1b	2.20 dd (3.0, 14.4)	2.48 dd (3.2, 14.4)			
2	4.10 d (3.0)	4.20 d (3.2)	3.34 dd (2.0, 4.0)	3.26 s	3.82 t (6.4)
3	3.20 br s	3.30 d (3.2)	3.52 br s	3.76 s	3.67 d (6.4)
5	1.22 dd (4.2, 12.0)	1.40 dd (6.8, 10.4)	1.06 m overlapped	1.42 dd (4.2, 12.0)	1.53 dd (4.0, 12.8)
6a	2.07 m	2.11 m	1.91 m	1.80 m	1.90 m
6b					2.08 m
7	5.43 d (3.6)	5.40 s	5.50b rs	5.50 d (3.6)	5.43 s
9	1.81 m overlapped	2.22 m	2.13 br s	2.23 br d (12.6)	2.27 m
11a	1.40 d (12.0)	3.18 d (4.0)	1.51 q (12.8)	1.50 q (12.6)	1.67 t (12.8)
11b	1.78 t (5.4, 12.0)		1.96 m	1.93 m	2.12 m
12	3.50 dd (4.2, 12.6)	2.90 d (3.6)	3.57 dd (4.4, 11.6)	3.55 dd (4.2, 12.0)	3.64 s
14a	1.99 m	1.62 m	2.04 m	2.03 m	1.77 d (13.6)
14b		2.26 m			2.54 d (13.6)
15	5.74 dd (10.8, 17.4)	5.94 dd (10.8, 17.6)	5.79 dd (10.8, 17.6)	5.76 dd (10.8, 17.4)	5.83 dd (10.4, 17.6)
16a	5.14 d (17.4)	5.08 d (10.8)	5.18 d (17.6)	5.15 d (17.4)	5.09 d (17.6)
16b	5.15 d (10.8)	5.16 d (17.6)	5.20 d (10.8)	5.17 d (10.8)	5.16 d (10.4)
17	0.88 s	1.02 s	0.93 s	0.91 s	0.90 s
18	1.00 s	1.02 s	0.94 s	1.01 s	0.94 s
19	1.10 s	1.10 s	1.02 s	0.88 s	1.11 s
20	1.10 s	1.17 s	1.04 s	1.02 s	0.99 s

[a] Recorded at 400 MHz for ^{1}H NMR.
[b] Recorded at 600 MHz for ^{1}H NMR.
[c] Recorded at 800 MHz for ^{1}H NMR.

2. Materials and methods

2.1. General experimental procedures

The melting points of crystals were measured by using a micro-melting point apparatus with an X-4 digital display system. The measurement of optical rotations was carried out by a PerkinElmer model 341 polarimeter. A Bruker Tensor spectrometer was used to obtain IR spectra. An Olis DSM-1000 spectrometer recorded the electronic circular dichroism (ECD) curves. A Shimadzu UV-260 spectrophotometer was used to collect UV spectra. ^{1}H, ^{13}C and 2D NMR spectra were acquired by the Bruker AVANCE III-400 or Bruker AVANCE III-800 or Varian Mercury-600BB spectrometers. A Bruker Daltonics APEX II spectrometer gave the HRESIMS data. X-ray diffraction analysis was collected on a SuperNova, Dual, Eos diffractometer with the Cu Kα radiation. The compounds were isolated from plants by microporous resin, silica gel column chromatography (CC), MCI gel CC, LiChroprep RP-C_{18} gel CC, Sephadex LH-20, and semi-preparative HPLC with a reversed-phase C_{18} column.

2.2. Plant materials

The roots of *E. hylonoma* were collected in June 2018 from Longnan City, Gansu Province, China, which was identified by Professor Zhao-Hui Huang of Agriculture and Forestry Technology College, Longnan Normal College. A voucher specimen of this plant (EH20180601) was deposited in the Natural Organic Academy of State Key Laboratory of Lanzhou University.

2.3. Extraction and isolation

The roots of *E. hylonoma* (8.0 kg) were extracted with 95% EtOH (3 × 50 L) at room temperature. The solvent was evaporated under reduced pressure to give a residue (786 g) that was suspended in water. Then the aqueous solution was partitioned with EtOAc and *n*-BuOH, successively. The EtOAc fraction (204 g) was subjected to macroporous resin (H_2O/EtOH, 70:30, 50:50, 20:80, 5:95, v/v) to afford four crude fractions (Fr.1–Fr.4). The Fr.3 (80 g) was applied to a silica gel column chromatography (CC) and eluted with petroleum ether/acetone (10:1, 5:1, 2:1, v/v) to produce three fractions (Fr.3.1–Fr.3.3). Fr.3.1 (8 g) was chromatographically separated on a silica gel CC and eluted with a gradient of petroleum ether/ethyl acetate (from 20:1 to 5:1, v/v) to afford compounds **11** (12.5 mg) and **13** (5.7 mg). Fr.3.1.3 (3.6 g) was applied to Sephadex LH-20 ($CHCl_3$/MeOH, 1:1) and reversed-phase semi-preparative HPLC (MeCN/H_2O) to yield compounds **10** (2.6 mg) and **8** (2.2 mg). Fr.3.2 (34 g) was subjected to an MCI gel CC and eluted with a gradient of MeOH/H_2O (from 20:80 to 100:0, v/v) to yield Fr.3.2.1–3.2.10. Compounds **1** (7.7 mg), **3** (2.3 mg), and **4** (3.9 mg) were isolated from Fr.3.2.4 (11 g) by repeated reversed-phase (RP) C_{18} gel CC and reversed-phase semi-preparative HPLC (MeOH/H_2O). Fr.3.2.5 (6 g) was applied to Sephadex LH-20 (MeOH) and reversed-phase semi-preparative HPLC (MeOH/H_2O) to afford compounds **2** (11.4 mg), **5** (5.2 mg), and **9** (13.4 mg). Compounds **12** (9.3 mg), **14** (7.8 mg), and **18** (3.7 mg) were isolated based on repeated silica gel CC and RP-C_{18} gel CC from Fr.3.2.6 (5 g). Fr.3.3 (13 g) was subjected to RP-C_{18} gel CC, eluted with a gradient system of MeOH/H_2O (from 20:80 to 100:0, v/v) to yield Fr.3.3.1–3.3.9. Compounds **6** (1.3 mg) and **7** (1.6 mg) were obtained by the further purification of Fr.3.3.3 (3.7 g) on repeated silica gel CC and reversed-phase semi-preparative HPLC (MeOH/H_2O). The Fr.3.3.4 (2.1 g) was separated on silica gel CC with a gradient of petroleum ether/ethyl acetate (from 10:1 to 2:1, v/v) as elution to obtain compounds **15** (5.6 mg), **16** (7.3 mg), and **17** (5.3 mg).

2.4. Compound characterization

(2R,3S,12S)-2,3,12-Trihydroxy-ent-isopimara-7,15-diene ***(1)***, colorless needle crystals (in CH_3OH); mp 197–200 °C, $[\alpha]_D^{22}$ −15.7 (c 0.19, MeOH); IR (KBr) ν_{max} 3382, 1363, 1264, 1068, 1034, 738, 704 cm^{-1}; ECD Δε, 205 (+18.6), 219 (−1.1); UV (MeOH) λmax (log ε) 198 (0.507), 202 (0.683) nm; ^{1}H NMR (600 MHz, $CDCl_3$) and ^{13}C NMR data (100 MHz, $CDCl_3$), see Tables 1 and 3; HRESIMS: *m/z* 343.2247, $[M+Na]^+$ (calcd for $C_{20}H_{32}O_3Na$, 343.2244).

(2R,3S,11R,12S)-2,3-Dihydroxy-11,12-epoxy-ent-isopimara-7,15-diene ***(3)***, colorless oil; $[\alpha]_D^{20}$ −31.1 (c 0.23, MeOH); IR (KBr) ν_{max} 3424, 2963, 2927, 2853, 1265, 739, 704 cm^{-1}; ECD Δε, 207 (+12.8), 224 (−1.1); UV (MeOH) λmax (log ε) 196 (0.615) nm; ^{1}H NMR (400 MHz,

$CDCl_3$) and ^{13}C NMR data (100 MHz, $CDCl_3$), see Tables 1 and 3; HRESIMS: *m/z* 341.2084, $[M+Na]^+$ (calcd for $C_{20}H_{30}O_3Na$, 341.2087).

(1R,2S,3S,12S)-1,2-Epoxy-3,12-dihydroxy-ent-isopimara-7,15-diene ***(4)***, colorless oil; $[\alpha]_D^{20}$ −5.0 (c 0.40, MeOH); IR (KBr) ν_{max} 3404, 2966, 2927, 1265, 1050, 1001, 737 cm^{-1}; ECD Δε, 200 (+29.0), 219 (−1.7); UV (MeOH) λmax (log ε) 197 (0.745), 201 (0.834) nm; ^1H NMR (400 MHz, $CDCl_3$) and ^{13}C NMR data (100 MHz, $CDCl_3$), see Tables 1 and 3; HRESIMS: *m/z* 341.2101, $[M+Na]^+$ (calcd for $C_{20}H_{30}O_3Na$, 341.2087).

(1R,2S,3R,12S)-1,2-Epoxy-3,12-dihydroxy-ent-isopimara-7,15-diene ***(5)***, colorless oil; $[\alpha]_D^{22}$ −27.78 (c 0.25, MeOH); IR (KBr) ν_{max} 3404, 2962, 2925, 2872, 1664, 1638, 1436, 1383, 1266, 1046, 997, 912, 737, 700 cm^{-1}; ECD Δε, 202 (+56.0), 217 (−5.5); UV (MeOH) λmax (log ε) 197 (0.579), 202 (0.843) nm; ^1H NMR (400 MHz, $CDCl_3$) and ^{13}C NMR data (100 MHz, $CDCl_3$), see Tables 1 and 3; HRESIMS: *m/z* 319.2275, $[M+H]^+$ (calcd for $C_{20}H_{31}O_3$, 319.2268).

(1R,2S,3S,12R)-1,2,3,12-Tetrahydroxy-ent-isopimara-7,15-diene ***(6)***, colorless oil; $[\alpha]_D^{24}$ −15.75 (c 0.13, MeOH); IR (KBr) ν_{max} 3392, 2923, 2855, 2372, 1384, 1257, 1157, 1112, 785 cm^{-1}; ECD Δε, 207 (+9.5), 223 (−1.7); UV (MeOH) λmax (log ε) 195 (0.481), 202 (0.758) nm; ^1H NMR (800 MHz, $CDCl_3$) and ^{13}C NMR data (200 MHz, $CDCl_3$), see Tables 1 and 3; HRESIMS: *m/z* 359.2207, $[M+Na]^+$ (calcd for $C_{20}H_{32}O_4Na$, 359.2193).

(1R,2S,3R,12R)-1,2,3,12-Tetrahydroxy-ent-isopimara-7,15-diene ***(7)***, colorless oil; $[\alpha]_D^{23}$ −25.48 (c 0.16, MeOH); IR (KBr) ν_{max} 3379, 2923, 2856, 2370, 1459, 1384, 1262, 1117, 783, 739 cm^{-1}; ECD Δε, 207 (+14.0), 223 (−0.8); UV (MeOH) λmax (log ε) 196 (0.429), 201 (0.711) nm; ^1H NMR (800 MHz, $CDCl_3$) and ^{13}C NMR data (200 MHz, $CDCl_3$), see Tables 2 and 3; HRESIMS: *m/z* 359.2205, $[M+Na]^+$ (calcd for $C_{20}H_{32}O_4Na$, 359.2193).

(2S,12R)-2,12-Dihydroxy-ent-isopimara-7,15-dien-3-one ***(8)***, colorless oil; $[\alpha]_D^{23}$ −8.9 (c 0.22, MeOH); IR (KBr) ν_{max} 3401, 2925, 2371, 1708, 1384, 1264, 1110, 1056, 739 cm^{-1}; ECD Δε, 205 (+6.8), 222 (−3.3), 277 (+1.0); ^1H NMR (600 MHz, $CDCl_3$) and ^{13}C NMR data (100 MHz, $CDCl_3$), see Tables 2 and 3; HRESIMS: *m/z* 319.2266, $[M+H]^+$ (calcd for $C_{20}H_{30}O_3H$, 319.2268).

3α,12β-Dihydroxy-ent-isopimara-8,15-dien-11-one ***(9)***, colorless oil; $[\alpha]_D^{23}$ −65 (c 0.31, MeOH); IR (KBr) ν_{max} 3445, 2963, 2929, 1709, 1655, 1609, 1458, 1368, 1254, 1130, 1098, 1025, 736 cm^{-1}; ECD Δε, 202 (+10.81), 248 (−17.46), 324 (+7.40); UV (MeOH) λmax (log ε) 249 (0.224) nm; ^1H NMR (400 MHz, $CDCl_3$) and ^{13}C NMR data (100 MHz, $CDCl_3$), see Tables 2 and 3; HRESIMS *m/z* 319.2271 $[M+H]^+$ (calcd for $C_{20}H_{30}O_3H$, 319.2268).

(12R,13R,15R)-2,15-Dihydroxy-12,16-epoxy-12-methoxy-ent-isopimara-1,7-dien-3-one ***(10)***, colorless crystals, mp 169–172 °C; $[\alpha]_D^{25}$ +3.82 (c 0.26, MeOH); IR (KBr) ν_{max} 3435, 2972, 2854, 1707, 1673, 1382, 1266, 1053, 738, 702 cm^{-1}; ECD Δε, 204 (+14.92), 234 (−2.04), 274 (+1.71), 326 (+1.87); UV (MeOH) λmax (log ε) 229 (0.371), 259 (0.323) nm; ^1H NMR (800 MHz, $CDCl_3$) and ^{13}C NMR data (200 MHz, $CDCl_3$), see Tables 2 and 3; HRESIMS: *m/z* 385.1998 $[M+Na]^+$ (calcd for $C_{21}H_{30}O_5Na$, 385.1985).

ent-Rosa-1(10),15-dien-2-one ***(11)***, colorless crystals, mp 112–113 °C; $[\alpha]_D^{22}$ +47.08 (c 1.32, MeOH); IR (KBr) ν_{max} 2965, 2932, 1669, 1609, 1467, 1380, 1305, 1205, 1157, 906, 736 cm^{-1}; ECD Δε 218 (−11.1), 242 (+9.3), 276 (−2.0), 320 (+1.3); UV (MeOH) λmax (log ε) 210 (0.186), 244 (0.626) nm; ^1H NMR (400 MHz, $CDCl_3$) and ^{13}C NMR data (100 MHz, $CDCl_3$), see Tables 2 and 3; HRESIMS: *m/z* 287.2370 $[M+H]^+$ (calcd for $C_{20}H_{30}OH$, 287.2369).

2.5. X-ray diffraction analysis.

All crystallographic data of the compounds **1**, **10**, and **11** have been deposited in the Cambridge Crystallographic Data Centre.

Crystal Data for ***1***. (CCDC 1885691) $C_{20}H_{32}O_3$, $M = 320.46$, $T = 295.66(10)$ K, crystal system: monoclinic, space group: C2, $a = 32.315(3)$ Å, $b = 6.04763(18)$ Å, $c = 24.8549(19)$ Å, $\alpha = 90.00°$,

Table 2
^1H NMR data of compounds **6–10** in $CDCl_3$.

Position	δ_H (*J* in Hz)				
	7[c]	**8**[b]	**9**[a]	**10**[c]	**11**[a]
1a	3.73 s	1.33 t (13.6)	3.06 br d (13.6)	6.19 s	6.01 d (2.0)
1b		2.47 dd (6.0, 12.8)	1.14 m		
2	4.23 s	4.57 m	1.72 m		
3a					2.18 d (15.6)
3b	3.54 s		3.26 dd (5.2, 11.6)		2.36 d (15.6)
5	1.74 dd (2.4, 11.2)	1.59 dd (2.8, 8.0)	1.00 m	1.85 dd (3.2, 12.0)	2.55 m
6a	1.97 br d (13.6)	2.15 m	1.44 m	1.98 m	1.44 m
6b	2.07 br d (13.6)	1.96 m	1.75 m	2.07 m	1.84 m
7a	5.43 d (3.2)	5.47 d (3.6)	2.25 m	5.55 d (4.8)	1.34 m
7b					1.72 m
8					1.77 m
9	2.89 d (12.0)	2.19 m overlapped		2.13 d (4.0)	
11a	1.64 m	1.63 d (10.0)		1.34 t (13.6)	1.53 m
11b		1.91 m		2.30 dd (5.6, 13.6)	1.74 m
12	3.66 s	3.66 br s	3.82 s		1.22 m
14a	1.80 d (13.6)	1.83 d (13.2)	2.36 m	1.84 dd (3.2, 14.4)	1.35 m
14b	2.59 d (13.6)	2.58 d (13.2)		1.88 d (14.4)	1.55 m
15	5.84 dd (11.2, 17.6)	5.83 dd (10.8, 17.6)	5.74 dd (10.8, 17.6)	3.63 dd (6.4, 12.0)	5.77 dd (10.8, 17.6)
16a	5.09 d (17.6)	5.12 d (17.6)	4.99 d (17.6)	3.77 dd (0.8, 10.4)	4.89 d (10.8)
16b	5.15 d (11.2)	5.20 d (10.8)	5.06 d (10.8)	4.32 dd (5.6, 10.4)	4.96 d (17.6)
17	0.91 s	0.91 s	1.27 s	1.05 s	0.98 s
18	1.01 s	1.16 s	1.04 s	1.20 s	1.09 s
19	1.14 s	1.19 s	0.84 s	1.17 s	0.83 s
20	1.04 s	1.20 s	1.09 s	1.08 s	1.01 s
OCH_3				3.29 s	
2-OH				6.01 d (1.6)	
15-OH				3.12 d (12.0)	

[a] Recorded at 400 MHz for ^1H NMR.
[b] Recorded at 600 MHz for ^1H NMR.
[c] Recorded at 800 MHz for ^1H NMR.

Table 3
^{13}C NMR data of compounds **1–10** in $CDCl_3$.

Position	δ_c (ppm)									
	1[a]	**3**[a]	**4**[a]	**5**[a]	**6**[b]	**7**[b]	**8**[a]	**9**[a]	**10**[b]	**11**[a]
1	43.3	42.0	61.0	58.0	75.6	76.0	47.8	34.8	123.4	122.6
2	70.8	71.0	58.0	56.7	72.9	74.2	68.8	27.9	143.6	200.5
3	78.2	78.1	76.0	72.9	75.6	79.0	216.3	78.4	200.5	53.3
4	37.7	38.1	34.5	36.0	36.7	36.7	47.1	39.0	43.4	36.7
5	49.7	49.0	49.7	42.3	44.7	40.1	52.6	52.2	48.1	44.5
6	23.1	23.2	22.4	22.1	23.5	23.2	23.6	17.8	22.7	17.6
7	122.6	122.9	124.0	124.1	121.2	120.7	120.8	35.1	122.6	24.8
8	133.0	130.2	133.3	133.5	134.9	134.6	134.7	155.7	133.1	30.7
9	51.5	50.2	46.2	46.1	46.1	37.0	44.7	139.5	45.2	38.5
10	34.3	34.3	34.5	34.5	39.8	38.6	35.4	38.2	36.0	175.4
11	27.6	53.1	27.7	27.7	27.8	26.1	25.8	198.0	24.7	34.0
12	74.3	60.7	74.0	74.0	72.9	73.0	72.3	80.2	109.2	39.6
13	42.4	37.9	42.8	42.8	41.7	41.6	41.6	42.7	48.6	36.0
14	45.2	39.2	45.6	45.7	37.7	37.8	37.1	43.1	43.0	32.4
15	146.5	145.3	146.2	146.3	145.9	146.0	145.6	138.2	78.8	150.4
16	113.7	112.2	114.2	114.4	113.9	113.7	114.1	114.9	75.4	109.1
17	13.7	20.3	13.8	13.8	23.1	23.0	23.0	25.6	14.0	22.0
18	29.9	29.4	28.6	21.7	26.4	28.7	25.0	28.3	25.3	28.8
19	17.3	16.5	17.2	28.0	23.0	22.9	22.5	15.8	22.5	19.9
20	16.5	16.8	13.2	13.2	10.8	15.7	15.5	19.1	16.0	18.8
OCH_3									47.7	

[a] Recorded at 100 MHz for ^{13}C NMR.
[b] Recorded at 200 MHz for ^{13}C NMR.

$\beta = 129.471(13)^\circ$, $\gamma = 90.00^\circ$, $V = 3749.6(4)$ Å^3, $Z = 8$, $D_{calc} = 1.135$ g/cm^3, μ (CuKα) = 0.557 mm^{-1}, $F(0\,0\,0) = 1408.0$, single crystal size: 0.14 × 0.12 × 0.07 mm^3, 13,600 reflections measured ($7.08^\circ \le 2\Theta \le 133.18^\circ$), 6422 unique ($R_{int} = 0.0271$, $R_{sigma} = 0.0363$) which were used in all calculations. The final R_1 was 0.0891 ($I \ge 2\sigma$ (I)) and wR_2 was 0.2783 (all data). Flack parameter = 0.0(4).

Crystal Data for ***10****.* (CCDC 1885700) $C_{21}H_{30}O_5$, $M = 362.45$, $T = 292.37(17)$ K, crystal system: orthorhombic, space group: $P2_12_12_1$, $a = 11.97578(16)$ Å, $b = 12.36669(19)$ Å, $c = 13.01505(19)$ Å, $\alpha = 90.00^\circ$, $\beta = 90.00^\circ$, $\gamma = 90.00^\circ$, $V = 1927.54(5)$ Å^3, $Z = 4$, $D_{calc} = 1.249$ g/cm^3, μ (CuKα) = 0.711 mm^{-1}, $F(0\,0\,0) = 784.0$, single crystal size: 0.18 × 0.16 × 0.13 mm^3, 15,451 reflections measured ($9.866^\circ \le 2\Theta \le 133.198^\circ$), 3386 unique ($R_{int} = 0.0235$, $R_{sigma} = 0.0176$) which were used in all calculations. The final R_1 was 0.0314 ($I \ge 2\sigma$ (I)) and wR_2 was 0.0884 (all data). Flack parameter = 0.10(7).

Crystal Data for ***11****.* (CCDC 1885690) $C_{20}H_{30}O$, $M = 286.44$, $T = 173.00(10)$ K, crystal system: orthorhombic, space group: $P2_12_12_1$, $a = 7.79565(13)$ Å, $b = 8.98011(15)$ Å, $c = 24.3461(4)$ Å, $\alpha = 90.00^\circ$, $\beta = 90.00^\circ$, $\gamma = 90.00^\circ$, $V = 1704.37(5)$ Å^3, $Z = 4$, $D_{calc} = 1.116$ g/cm^3, μ (CuKα) = 0.498 mm^{-1}, $F(0\,0\,0) = 632.0$, single crystal size: 0.17 × 0.15 × 0.12 mm^3, 5415 reflections measured ($11.92^\circ \le 2\Theta \le 133.1^\circ$), 2868 unique ($R_{int} = 0.0203$, $R_{sigma} = 0.0237$) which were used in all calculations. The final R_1 was 0.0368 ($I \ge 2\sigma$ (I)) and wR_2 was 0.0982 (all data). Flack parameter = −0.10(4).

2.6. Cell culture and nitric oxide inhibitory assay

RAW264.7 macrophage cell lines were purchased from the Cell Bank of the Chinese Academy of Sciences, Shanghai, China. The cells were cultured in Dulbecco's modified Eagle's medium (DMEM) supplemented with 10% (v/v) fetal calf serum, 100 μg/mL streptomycin and 100 μg/mL penicillin G at 37 °C in a fully humidified atmosphere with 5% CO_2. The cells were harvested with trypsin and diluted to a suspension in fresh medium. Then cells were seeded in 96-well plates with 1×10^5 cells/well and allowed to adhere for 2 h. The tested compounds were dissolved in DMSO, and then diluted with DMEM to make the final DMSO concentration < 0.1%.

After that, the cells were incubated with fresh medium, containing LPS (10 μg/ml). Then the various concentrations of test compounds were added in 96-well plates and then co-incubated for 24 h. The NO production induced by LPS in RAW264.7 macrophages cells was determined by measuring the accumulation of nitrite in the culture supernatant with Griess reagent. Briefly, 60 μl of the supernatant from each well of 96-well plates was reacted with an equal volume of Griess reagent and then allowed to stand for 10 min at room temperature. The absorbance at 540 nm was measured using a Microplate Reader. The nitrite concentration in the medium was determined from the calibration curve obtained by using different concentrations of sodium nitrite ($NaNO_2$) in the culture medium as standard. The blank correction was carried out by subtracting the absorbance due to medium only from the absorbance reading of each well [14].

Besides, the MTT method [15] was used to determine whether the inhibition of NO production was due to the cytotoxicity of the tested compounds.

2.7. Western blotting analysis

Western blotting analysis for the iNOS expressions was carried out according to the method reported in literature [2,16]. Briefly, RAW264.7 macrophage cells were seeded at 3×10^5 cells/well in 6-well culture plates and incubated for 12 h. Then the cells were stimulated with LPS (10 μg/ml) for 24 h, and treated with compounds **2** and **12** for 24 h, respectively. Then, the cells were successively washed with cold PBS twice and lysed with lysis buffer. Subsequently, the lysates were centrifuged and the supernatants were collected to acquire the total protein. Concentrated proteins were separated by 12% SDS-polyacrylamide gel (SDS-PAGE) and then transferred to polyvinylidene difluoride (PVDF) membranes. The PVDF membrane was incubated with a 1:1000 dilution of iNOS antibody overnight at 4 °C. After being washed with TBST for 30 min, the membranes were incubated with appropriate secondary antibodies for 1 h at room temperature and then washed with TBST for 30 min. Finally, the protein blots were incubated with the ECL reagents (Beyotime, Jiangsu province, People's Republic of China) and then detected. GAPDH protein was used as an internal reference.

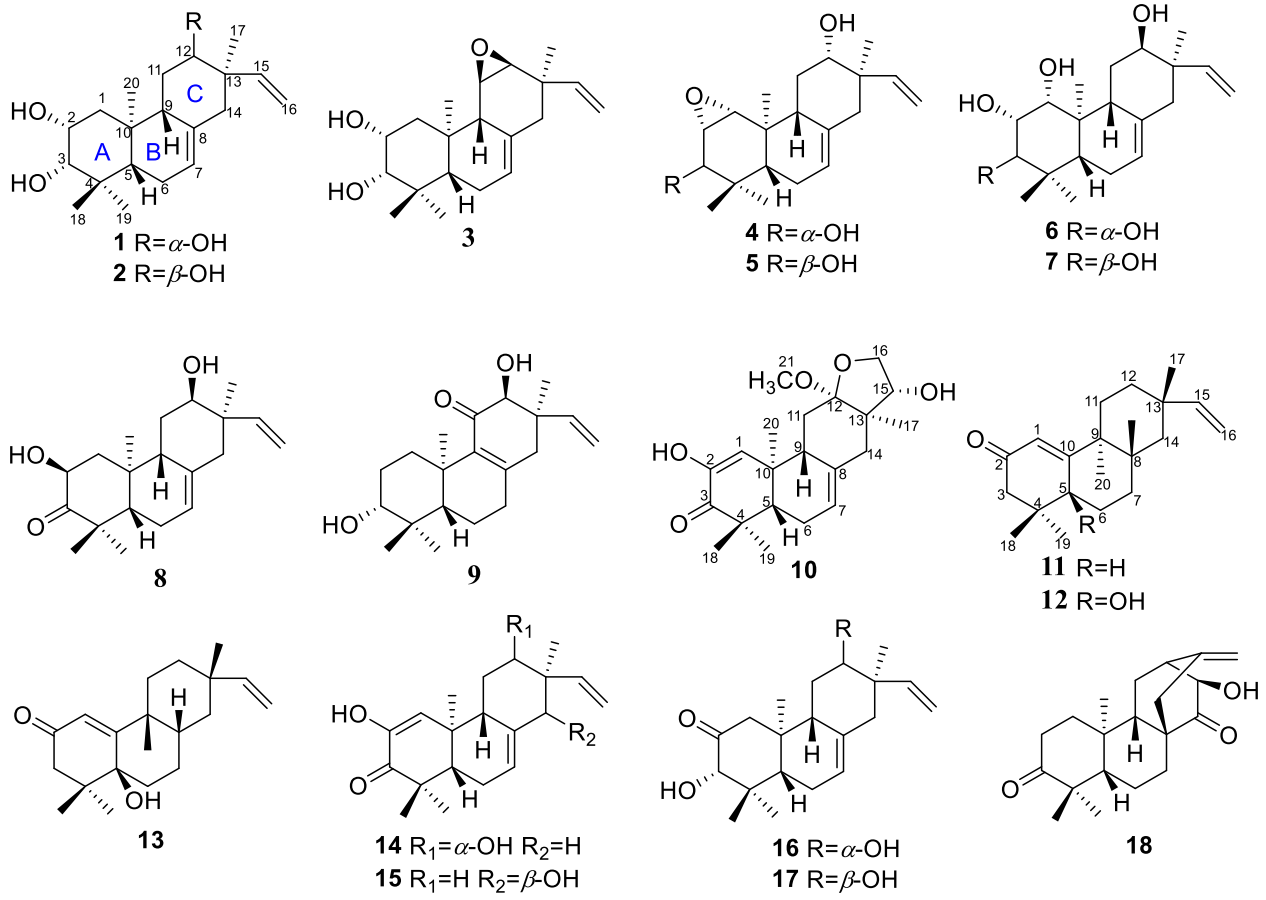

Fig. 1. Structures of compounds **1–18**.

2.8. Statistical analysis

Tests were conducted in triplicate and the results were expressed as the means ± standard deviation (SD) (n = 3). The statistical comparisons were analyzed by a one-way analysis of variance (ANOVA). The mean values were compared using Student's *t* test. P value less than 0.05 was considered statistically significant.

3. Results and discussion

3.1. Structure elucidation

The phytochemical investigation of *Euphorbia hylonoma* led to the isolation of 18 diterpenoids (**1–18**), including nine new *ent*-isopimarane (**1** and **3–10**), a new *ent*-rosane (**11**), and eight known diterpenoids (**2** and **12–18**). The known compounds were successively identified as euphorbesulin P (**2**) [17], euphorpekone A (**12**) [18], euphorpekone B (**13**) [18], (12*β*)-2,12-dihydroxyisopimara-1,7,15-trien-3-one (**14**) [19], yuexiandajisu C (**15**) [20], (3*β*,12*β*)-3,12-dihydroxyisopimara-7,15-dien-2-one (**16**) [19], (3*β*,12*α*)-3,12-dihydroxypimara-7,15-dien-2-one (**17**) [21], antiquorin (**18**) [22] (Fig. 1).

Compound **1**, needle crystals (in CH_3OH), was established a molecular formula of $C_{20}H_{32}O_3$ based on the HRESIMS (*m/z* 343.2247, $[M+Na]^+$, calcd for $C_{20}H_{32}O_3Na$, 343.2244) and ^{13}C NMR data, accounting for five indices of hydrogen deficiency (IOHD). In its IR spectrum, an absorption band at 3382 cm^{-1} indicated the presence of hydroxy groups. The ^1H NMR spectrum (Table 1) exhibited signals for vinylic protons [δ_H 5.74 (dd, J = 10.8, 17.4 Hz), 5.15 (d, J = 10.8 Hz), and 5.14 (d, J = 17.4 Hz)], an olefinic proton at δ_H 5.43 (d, J = 3.6 Hz), three oxymethine protons [δ_H 4.10 (d, J = 3.0 Hz), 3.50 (dd, J = 4.2, 12.6 Hz), and 3.20 (br s)], and four tertiary methyls at δ_H 0.88, 1.00, 1.10, and 1.10. The ^{13}C NMR and HSQC spectra showed 20 carbon resonances (Table 3), corresponding to four methyls, five methylenes (one olefinic carbon), seven methines (two olefinic carbons and three oxygenated carbons), and four quaternary carbons (one olefinic carbon). Apart from two double bonds, the remaining degrees of unsaturation were assumed to represent a tricyclic skeleton. All above data were reminiscent of known compound **2**, except for the difference of the coupling pattern of H-12 observed in their ^1H NMR spectra [δ_H 3.50 (dd, J = 4.2, 12.6 Hz) in **1** and δ_H 3.66, brs in **2**]. Analysis of $^1H-^1H$ COSY and HMBC spectra (Fig. 2a) completed the assignment of the planar structure of **1** which was the same as that of **2**.

In the NOESY spectrum (Fig. 2b), the cross-peaks of H-3 with H-5 and Me-18, of H-9 with H-5 and H-12, and of H-12 with H-15 indicated that H-5, H-9, H-15, and Me-18 were *β*-oriented and that Me-17, Me-19, Me-20, OH-3, and OH-12 were *α*-oriented. The small coupling constant values of $J_{1,2}$ = 3.0 Hz and $J_{2,3}$ = 0 Hz suggested that OH-2 was also *α*-oriented. Accordingly, compound **1** was the C-12 epimer of **2**. High quality single crystals of **1** were obtained by recrystallization and the X-ray diffraction analysis with Cu Kα radiation (Fig. 5) not only further confirmed its relative configuration but also established its absolute configuration as (2*R*, 3*S*, 5*S*, 9*R*, 10*S*, 12*S*, 13*R*) with Flack parameter of 0.0(4) and Hooft parameter of 0.04(15) [23,24].

The molecular formula of **3** was deduced as $C_{20}H_{30}O_3$ from the ^{13}C NMR data and a molecular ion peak $[M+Na]^+$ at *m/z* 341.2084 in the HRESIMS, with six IOHD. The 1D NMR spectra of **3** were comparable to those of **1**, with the main differences being the chemical shifts of C-11/H-11, C-12/H-12, C-13, and C-14/H-14 (Tables 1 and 3). The ^{13}C NMR resonances at δ_C 53.1 (C-11) and δ_C 60.7 (C-12) and the IOHD indicated the presence of an epoxy group at C-11 and C-12, which was further confirmed by the $^1H-^1H$ COSY correlations of H-9/H-11/H-12 and the HMBC cross-peaks from H-11 (δ_H 3.18, d, J = 4.0 Hz) to C-8, C-9, and

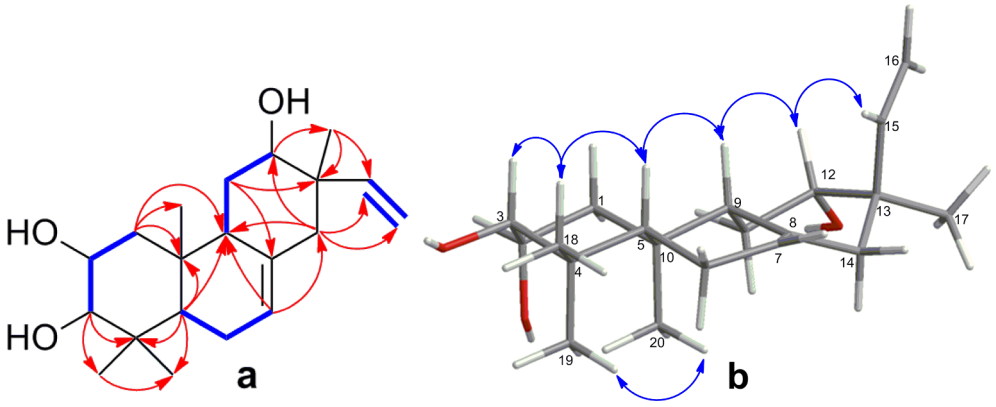

Fig. 2. (a) HMBC and $^{1}H-^{1}H$ COSY (b) NOESY correlations of compound **1**.

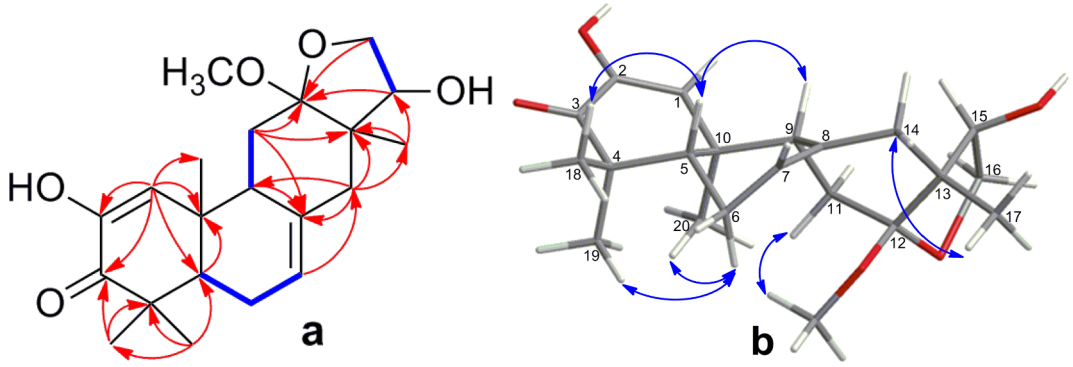

Fig. 3. (a) HMBC and $^{1}H-^{1}H$ COSY (b) NOESY correlations of compound **10**.

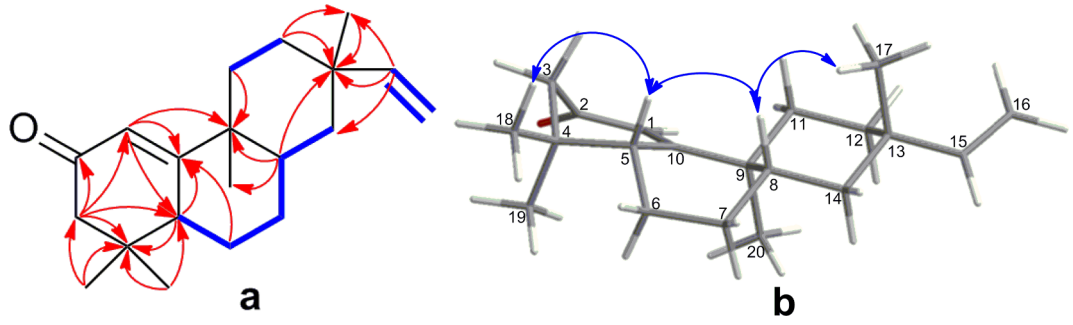

Fig. 4. (a) HMBC and $^{1}H-^{1}H$ COSY (b) NOESY correlations of compound **11**.

C-10, from H-12 (δ_H 2.90, d, J = 4.0 Hz) to C-13, from H-14, H-15, and H-17 to C-12. Simultaneously, the epoxy group was speculated to be in the β orientation based on the NOESY correlations of H-11/H-20, H-11/H-12, and H-12/H-17. The orientations of the hydroxy groups at C-2 and C-3 of **3** were the same as those of **1** according to their similar NOESY spectra. The ECD spectrum of **3** was similar to that of **1** (Fig. 6), which suggested that the absolute configuration of **3** was the same as that of **1**. Thus, the structure of **3** was established as shown in Fig. 1.

Compound **4** had the same molecular formula of $C_{20}H_{30}O_3$ as compound **3**, as identified by its HRESIMS (m/z 341.2101, $[M+Na]^+$) and ^{13}C NMR data. A detailed comparison of the 1D NMR spectra of **4** with those of **3** suggested that these two compounds were isomers. The significant differences were the positions of the epoxy and hydroxy groups. The HMBC signals of H-12 with C-17, of H-14, H-15, and H-17 with C-12 (δ_C 72.7) and the $C(9)H_1-C(11)H_2-C(12)H_1$ spin system verified that a hydroxy group was attached to C-12. The epoxy group at C-1 and C-2 and the other hydroxy group at C-3 were deduced from the $^{1}H-^{1}H$ COSY correlations of H-1/H-2/H-3 and the HMBC cross-peaks from H-1 to C-5, C-9, and C-10 and from H-3 to C-18 and C-19. The two hydroxy and epoxy groups were determined to be in the α orientation according to its NOESY correlations of H-1/H-9, H-3/H-5, H-5/H-9, and H-9/H-12, as well as the $J_{11,12}$ value of 4.4 and 11.6 Hz. Based on the similarities of the ECD curves of compounds **1**, **3**, and **4** (Fig. 6), the absolute configuration of **4** was assigned as (1*R*, 2*S*, 3*S*, 5*R*, 9*R*, 10*S*, 12*S*, 13*R*).

The HRESIMS data of compound **5** showed an $[M+H]^+$ ion at m/z 319.2275, attributable to a molecular formula of $C_{20}H_{30}O_3$, which was the same as compound **4**. The IR spectrum exhibited a characteristic absorption band at 3404 cm^{-1} for hydroxy groups. The 1D NMR data of **5** had high resemblance to those of **4**, except for the difference of chemical shifts and coupling patterns of H-1/C-1, H-2/C-2, and H-3/C-3 (Tables 1 and 3). Analysis of the $^{1}H-^{1}H$ COSY and HMBC spectra of **5** and **4** indicated these two compounds shared the identical planar structure. The NOESY signals of H-1/H-9, H-3/H-19, H-3/H-20, H-5/H-9, H-9/H-12, and H-12/H-15 proved that the C-3 hydroxy group was in the β orientation and that the C-12 hydroxy and epoxy groups were in the α orientation. Thus, compound **5** was identified as the C-3 epimer of **4**. The ECD curve of **5** was similar to those of **1**, **3**, and **4**, indicating that

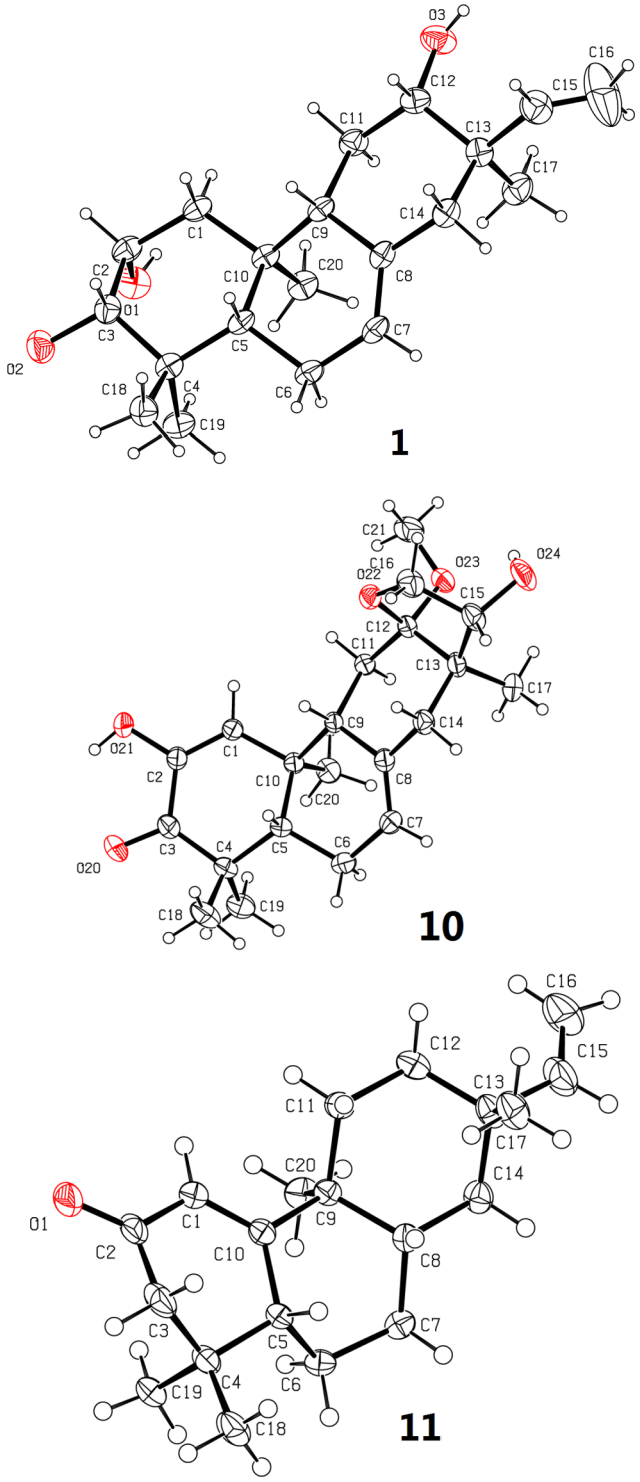

Fig. 5. ORTEP drawing of compounds **1**, **10**, and **11** (Cu Kα).

these compounds shared the similar absolute configuration. Accordingly, the structure of this compound was assigned as (1*R*,2*S*,3*R*,12*S*)-1,2-epoxy-3,12-dihydroxy-*ent*-isopimara-7,15-diene.

The molecular formula of **6** was assigned as $C_{20}H_{32}O_4$ based on the ^{13}C NMR data and a sodium adduct ion at *m/z* 359.2207 ($[M+Na]^+$) in the HRESIMS. Inspection of the 1D NMR data of **6** exhibited that its structure was closely related to that of **1**, with the exception of an additional oxygenated methine ($\delta_{H/C}$ 3.86/75.6) in **6** replacing a methylene in **1**. The HMBC cross-peaks from H-1 to C-9, from H-2 to C-1, C-3, and C-4, and from H-3 and H-20 to C-1 confirmed that this hydroxy

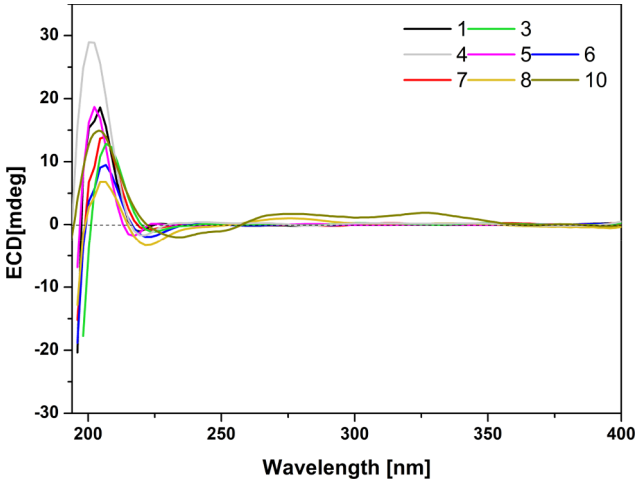

Fig. 6. The ECD spectra of compounds **1**, **3**–**8**, and **10** (solvent: MeOH).

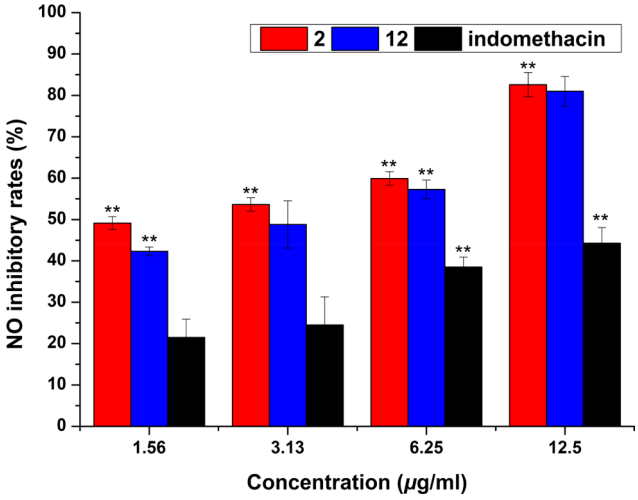

Fig. 7. The inhibitory effects of compounds **2**, **12** and positive control (indomethacin) against NO production induced by LPS in RAW 264.7 cells at different concentrations (**p < 0.01).

Table 4
Inhibition effects against NO production induced by LPS in RAW 264.7 cells of compounds **1**, **2**, **5**, **9**, and **11**–**18**.

Compounds	IC_{50} (μM)[a]
1	45.48 ± 6.23
2	7.12 ± 1.09
5	57.51 ± 9.10
9	> 100
11	48.40 ± 4.55
12	12.73 ± 2.28
13	41.30 ± 5.22
14	47.95 ± 3.12
15	41.34 ± 3.26
16	> 100
17	> 100
18	> 100
Indomethacin	41.41 ± 2.73

[a] The data represent the mean ± SD of three independent experiments.

group was attached to C-1. In addition, the coupling pattern of H-12 [δ_H 3.64, brs] in **6** differed from that of H-12 [δ_H 3.50 (dd, J = 4.2, 12.6 Hz)] in **1**, indicating that the C-12 hydroxy group in **6** was *β*-

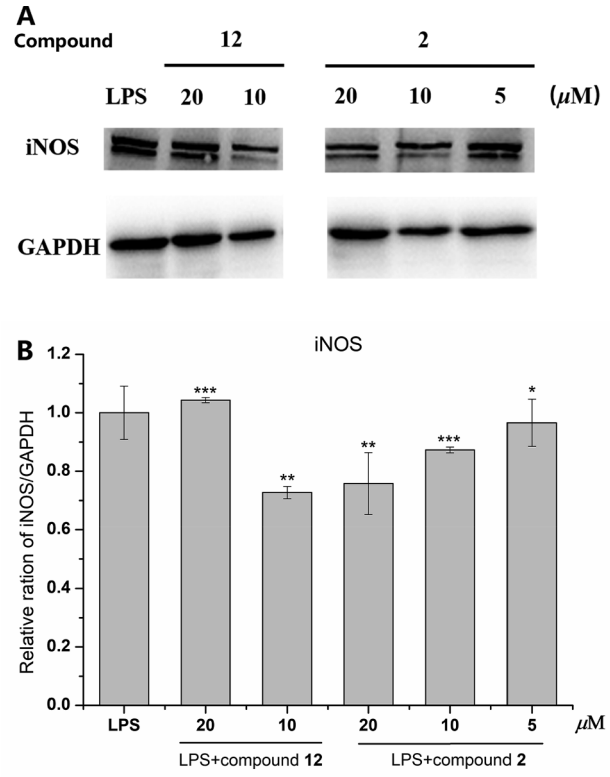

Fig. 8. Effects of compounds **2** and **12** on the iNOS protein expression in LPS-induced RAW264.7 cells. (A) Western blotting results of the iNOS protein levels. (B) Quantitative analysis of iNOS protein expression. GAPDH protein was used as internal reference. ***p < 0.001, **p < 0.01, *p < 0.05 compared with LPS-stimulated cells.

oriented. The NOESY data between H-12/H-17 further confirmed this deduction. The NOESY correlations of H-1/H-5, H-1/H-9, H-2/H-18, H-3/H-5, H-5/H-9, and H-5/H-18 indicated that the OH-1, OH-2, and OH-3 were all in the *α* orientation. Consequently, the similarities of the ECD spectra of compounds **1** and **6** indicated that they had the same absolute configuration.

Compound **7** showed an identical molecular formula of $C_{20}H_{32}O_4$ to compound **6**, as confirmed by its ^{13}C NMR and HRESIMS (*m/z* 359.2205, $[M+Na]^+$) data. The similar 1D NMR data for compounds **6** and **7** suggested that the structure of **6** resembled that of **7**, except for the orientation of the C-3 hydroxy group, as deduced from the coupling patterns of H-2 [δ_H 3.82 (t, J = 6.4 Hz) in **6** and δ_H 4.23, brs in **7**] and H-3 [δ_H 3.67 (d, J = 6.4 Hz) in **6** and δ_H 3.54, brs in **7**]. The NOESY correlations of H-1/H-5, H-2/H-5, H-2/H-18, H-1/H-9, H-5/H-18, H-3/H-19, H-3/H-20, H-9/H-14b, H-12/H-17, and H-14a/H-17 determined that compound **7** was the C-3 epimer of **6**. The ECD curve of **7** was consistent with those of **1** and **6**, suggesting the same absolute configuration for these three compounds.

The HRESIMS data of **8** displayed an $[M+H]^+$ ion at *m/z* 319.2266, consistent with a molecular formula of $C_{20}H_{30}O_3$. The IR spectrum showed absorption bands at 3401 and 1708 cm^{-1} indicative of hydroxy and carbonyl groups, respectively. Comparison of the ^1H and ^{13}C NMR spectra of **8** with those of **1** indicated that their structures were similar to each other, except for the replacement of a hydroxy group in **1** with a carbonyl group in **8**. The HMBC cross-peaks of H-1, H-2, H-18, and H-19 with C-3 (δ_C 216.3) verified that this carbonyl group was located at C-3. Analysis of the NOESY spectrum revealed that the C-2 and C-12 hydroxy groups were both *β*-oriented by the correlations of H-2/H-19, H-2/H-20, H-5/H-9, H-5/H-18, H-9/H-14b, H-12/H-14a, H-12/H-17, H-14a/H-17, and H-14b/H-16. The absolute configuration of **8** was proposed as depicted in Fig. 1 based on the biosynthetic considerations and the similar ECD curve to those of **1**, **3**, **4**, **5**, **6**, and **7** (Fig. 6).

Compound **9** was assigned a molecular formula of $C_{20}H_{30}O_3$ based on the HRESIMS (*m/z* 319.2271, $[M+H]^+$, calcd for $C_{20}H_{30}O_3H$, 319.2268) and ^{13}C NMR data. The 1D NMR data of **9** were comparable to those of **8**, except for the difference in chemical shift of the carbonyl group (δ_C 198.0, C-11) and the absence of an olefin proton signal in the ^1H NMR spectrum of **9**. The HMBC correlations from H-3 to C-2, C-4, C-18, and C-19, from H-12 to C-9, C-11, C-13, C-14, C-15 and C-17, and from H-14 to C-12 and the $C(1)H_2{-}C(2)H_2{-}C(3)H_1$ spin system showed two hydroxy groups attached to C-3 and C-12 and a carbonyl group located at C-11, respectively. The tetrasubstituted double bond was assigned between C-8 and C-9 based on the HMBC correlations of H-6 with C-8, of H-7 with C-8 and C-9, and of H_3-20 with C-9. The C-3 hydroxy group was determined to be *α*-oriented and the C-12 hydroxy group was *β*-oriented by the NOESY correlations of H-3/H-5, H-3/H_3-18, and H-12/H_3-17. Thus, the structure of **9** was established as 3*α*,12*β*-dihydroxy-*ent*-isopimara-8,15-dien-11-one.

Compound **10** was isolated as colorless crystals. Its molecular formula of $C_{21}H_{30}O_5$ was established by the HRESIMS (*m/z* 385.1998, $[M+Na]^+$, calcd for $C_{21}H_{30}O_5Na$, 385.1985) and ^{13}C NMR data, indicating seven degrees of unsaturation. The IR spectrum showed absorption bands at 3435 and 1673 cm^{-1}, indicative of hydroxy and carbonyl groups, respectively. Inspection of 1D NMR revealed that it was structurally similar to **14**. The obvious difference were the absence of the characteristic vinylic group and the presence of signals for a methoxy (δ_H 3.29; δ_C 47.7), an oxygenated methine [δ_H 3.63 (dd, J = 6.4, 12.0 Hz, H-15); δ_C 75.4], an oxygenated methylene [δ_H 3.77 (d, J = 10.4 Hz, H-16a), δ_H 4.32 (dd, J = 5.6, 10.4 Hz, H-16b); δ_C 78.8], an oxygen-bearing tertiary carbon (δ_C 109.2) and two hydroxy groups at

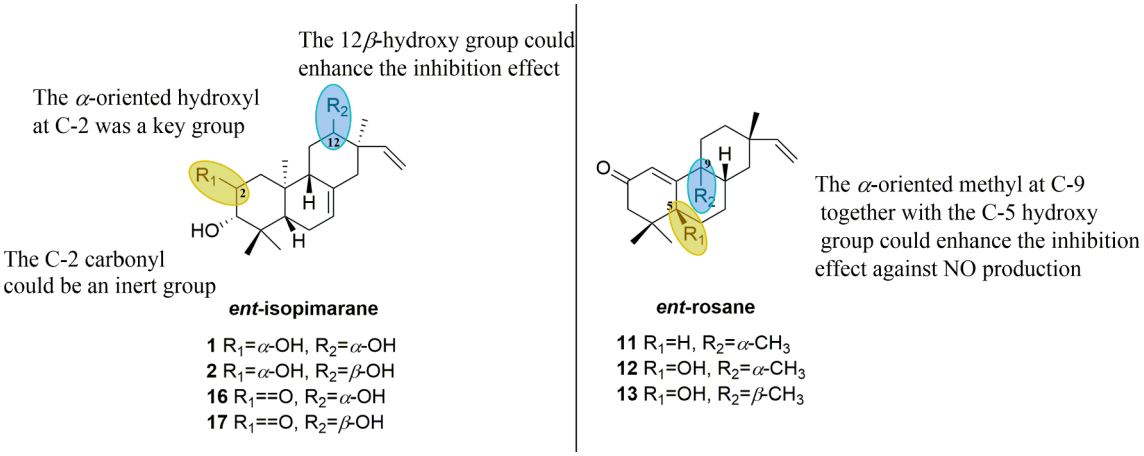

Fig. 9. The structure-activity relationships of diterpenoids.

δ_H 3.12 (d, J = 12.0 Hz) and δ_H 6.01 (d, J = 1.6 Hz) in **10**. Two double bonds [δ_H 6.19 (s, H-1); δ_C 123.4 and 143.6) and δ_H 5.55 (d, J = 4.8 Hz, H-7); δ_C 122.6 and 133.1)] and a carbonyl (δ_C 200.5) accounting for three degrees of unsaturation, the remaining ones suggested four rings present in compound **10**. Analysis of the 1D and 2D NMR data of **10** indicated the rings A, B and C were the same as those of **14**. The HMBC cross-peaks from H-16 to C-12 and from H-OCH_3 to C-12 and the chemical shift of C-12 (δ_C 109.2) implied the linkage between C-12 and C-16 via an oxygen atom to form a five-membered ring of the acetal moiety and simultaneously suggested the OCH_3 attached to C-12. The hydroxy group at δ_H 3.12 attached to C-15 was deduced from the $^1H-^1H$ COSY correlation of H-15/H-16 and the HMBC correlations of H-15 with C-12 and C-14, of H-17 with C-15, and of 15-OH with C-15 (Fig. 3a). The orientations of the OH at C-15 and OCH_3 at C-12 could not be determined from the NOESY spectrum due to the lack of the related signals (Fig. 3b). Otherwise, a single crystal was obtained and an X-ray diffraction analysis of Cu Kα radiation (Fig. 5) unambiguously permitted not only the relative configuration but also the assignment of the absolute configuration of **10** as (5*S*, 9*R*, 10*S*, 12*R*, 13*R*, 15*R*).

The HRESIMS analysis of **11** showed an $[M+H]^+$ ion at m/z 287.2370, consistent with a molecular formula of $C_{20}H_{30}O$. In the IR spectrum, an absorption band at 1669 cm^{-1} indicated the presence of carbonyl groups. Analysis of the 1D NMR data of **11** indicated that its structure resembled that of **12**, except for a methine (δ_H 2.55; δ_C 44.5) at C-5 in **11** replacing an oxygen-bearing tertiary carbon (δ_C 75.1) in **12**. This assignment was confirmed by the $^1H-^1H$ COSY correlation of H-5/H-6/H-7 and the HMBC cross-peaks from H-1, H-3, and H-6 to C-5 and from H-5 to C-1, C-2, C-4, C-7, and C-10 (Fig. 4a). The signals of H-5/H-18 and of H-8/H-17 observed in the NOESY spectrum (Fig. 4b) were not sufficient to define its relative configuration. Then, an X-ray crystallographic analysis with Cu Kα radiation (Fig. 5) was performed to confirm its structure and the absolute configuration as depicted in Fig. 2.

3.2. Nitric oxide inhibitory activity

Compounds **1**, **2**, **5**, **9**, and **11–18** were evaluated for their inhibitory effects on NO production induced by LPS in RAW 264.7 cells. The remaining compounds had not been evaluated due to the small amounts of compounds that were isolated. All the tested compounds showed no cytotoxicity against RAW 264.7 macrophages cells at their respective effective concentrations. Among these compounds, compounds **2** and **12** exhibited noteworthy inhibitory effects against NO production in a dose-dependent manner. And at each test concentrations, the inhibition rates of compounds **2** and **12** were greater than those of the positive control (indomethacin), as shown in Fig. 7. Meanwhile, the IC_{50} values for **2** and **12** were 7.12 and 12.73 μM, respectively, which were better than indomethacin (IC_{50} = 41.41 μM). In addition, compounds **1**, **5**, **11**, **13**, **14**, and **15** showed moderate inhibitory effects similar to indomethacin. However, compounds **9**, **16**, **17**, and **18** were less active for inhibiting the NO production with IC_{50} value > 100 μM (Table 4).

3.3. Effects on iNOS protein expression

It is well known that the pro-inflammatory mediator NO plays an important role in various inflammatory related diseases. NO is synthesized by three types of nitric oxide synthase (NOS): endothelial NOS (eNOS), neural NOS (nNOS), and inducible NOS (iNOS). And iNOS is involved in the regulation of excessive NO production in the inflammatory process. To investigate the mechanism of anti-inflammatory activity, the active compounds **2** and **12** for inhibiting NO production were selected to evaluate the effects on the iNOS protein expressions using Western blotting experiments. As shown in Fig. 8, compound **2** could weakly suppress the iNOS expression in a dose-dependent manner, and compound **12** had no inhibitory effect on the iNOS expression at a highest test concentration of 20 μM. It was speculated that the inhibition mechanism of NO production caused by compounds **2** and **12** may not be achieved by regulating the expression of levels of iNOS.

3.4. Structure-activity relationships (SAR)

Compound **2** (IC_{50} = 7.12 μM), an *ent*-isopimarane diterpenoid, was the C-12 epimer of **1** with the C-12 hydroxy group being β-oriented. But compound **1** showed moderate inhibitory effect with IC_{50} value of 45.48 μM. The above results indicated that the orientation of the C-12 hydroxy group could be responsible to affect their anti-inflammatory activity. Thus, it was very important to determine the configurations of each chiral center of compound for the development of new drugs. Sometimes the opposite effects may be resulted from the different configurations of the compound, such as (d or l)-etozolin.

Compound **12** was an *ent*-rosane diterpenoid (IC_{50} = 12.73 μM). Its structure was closely similar to those of **11** and **13**. However, compounds **11** and **13** displayed moderate inhibitory effects with IC_{50} values of 48.40 and 41.30 μM, respectively. The difference between **11** and **12** was the hydroxy group at C-5 in **12** replacing the hydrogen atom in **11**, which proved that the C-5 hydroxy group in **12** was an important group to enhance anti-inflammatory activity. Therefore, the different substituents could significantly affect the level of anti-inflammatory activity. A comparison of **12** with **13**, these two compounds had the same planar structure, except for the orientation of the methyl located at C-9. Accordingly, compound **12** was the C-9 epimer of **13**. The α-oriented methyl at C-9 in **12** could be crucial for inhibiting NO production, which also indicated the importance for determining the configuration of compound.

Analysis of the SARs of the compounds **16** vs **1** and **17** vs **2**, compounds **1** and **2** exhibited inhibitory effects with IC_{50} values of 45.48 and 7.12 μM, respectively. However, compounds **16** and **17** were less active for inhibiting the NO production (IC_{50} > 100 μM). The difference of these two pairs of compounds (**16** vs **1** and **17** vs **2**) was the C-2 carbonyl in **16** and **17** instead of the hydroxy group in **1** and **2**, respectively. The above results indicated that the carbonyl at C-2 in **16** and **17** could be an inert group for inhibiting the NO production.

Thus, compounds **2** and **12** should be considered as lead compounds for the development of new anti-inflammatory agents.

4. Conclusion

In summary, the phytochemical investigation of *E. hylonoma* led to the isolation of 18 diterpenoids (**1–18**), ten of which were new (**1** and **3–11**). Their structures were confirmed by extensive spectroscopic data, crystal X-ray diffraction analysis, and electronic circular dichroism. These compounds were evaluated for their inhibitory effects against NO production induced by LPS in RAW 264.7 cells. Among them, compounds **2** and **12** exhibited significant inhibitory effects against NO production. And the SARs of them were discussed as shown in Fig. 9. Thus, compounds **2** and **12** could offer promising lead structures with anti-inflammatory activity, which could be useful in the pharmaceutical industry. Meanwhile, *E. hylonoma* is a rich source for producing diterpenoids and for the development of new potential anti-inflammatory agents.

Acknowledgement

The financial support from the Natural Science Foundation of Gansu Province (18JR4RA003) is greatly acknowledged.

Appendix A. Supplementary material

1D and 2D NMR, IR spectra, HRESIMS of compounds **1** and **3 − 11**. Supplementary data to this article can be found online at https://doi.org/10.1016/j.bioorg.2019.103256.

References

[1] Q.G. Ma, R.R. Wei, M. Yang, X.Y. Huang, G.Y. Zhong, Z.P. Sang, J.H. Dong, J.C. Shu, J.Q. Liu, R. Zhang, J.B. Yang, A.G. Wang, T.F. Ji, Y.L. Su, Bioorg. Chem. 86 (2019) 159–165.
[2] Y.R. Xi, L.J. An, X.Y. Yang, Z.T. Song, J. Zhang, M. Tuerhong, D.Q. Jin, Y.S. Ohizumi, D.H. Lee, J. Xu, Y.Q. Guo, Bioorg. Chem. 87 (2019) 417–424.
[3] C.C. Chen, M.W. Lin, C.J. Liang, S.H. Wang, PLoS ONE 11 (2016) e0158662.
[4] A.R. Jassbi, Phytochemistry 67 (2006) 1977–1984.
[5] L.C.L. Bao, S.S. Na, World Chinese Med. 13 (2018) 2090–2094.
[6] İ. Yener, Ö.T. Ölmez, A. Ertas, M.A. Yilmaz, M. Firat, S.İ. Kandemir, M. Öztürk, U. Kolak, H. Temel, Ind. Crop. Prod. 123 (2018) 442–453.
[7] C.Y. Zhang, Y.L. Wu, P. Zhang, Z.Z. Chen, H. Li, L.X. Chen, J. Nat. Prod. 82 (2019) 756–764.
[8] P.X. Wang, C.F. Xie, L.J. An, X.Y. Yang, Y.R. Xi, S. Yuan, C.Y. Zhang, M. Tuerhong, D.Q. Jin, D. Lee, J. Zhang, Y. Ohizumi, J. Xu, Y.Q. Guo, J. Nat. Prod. 82 (2019) 183–193.
[9] Q.Q. Song, Y. Rao, G.H. Tang, Z.H. Sun, J.S. Zhang, Z.S. Huang, S. Yin, J. Med. Chem. 62 (2019) 2060–2075.
[10] W.J. Wei, Q.Y. Song, Z.Q. Zheng, X.J. Yao, Y. Li, K. Gao, J. Nat. Prod. 81 (2018) 2381–2391.
[11] Z.P. Mai, G. Ni, Y.F. Liu, Y.H. Li, L. Li, J.Y. Li, D.Q. Yu, J. Org. Chem. 83 (2018) 167–173.
[12] Z.P. Mai, G. Ni, Y.F. Liu, L. Li, J.Y. Li, D.Q. Yu, Org. Lett. 20 (2018) 3124–3127.
[13] Jiangsu New Medical College, Dictionary Traditional Drugs, Shanghai Scientific and Technical Publishers, Shanghai, 1993, p. 41.
[14] S. Awale, Y. Tezuka, A.H. Banskota, I.K. Adnyana, S. Kadota, J. Nat. Prod. 66 (2003) 255–258.
[15] C.P. Chiu, S.C. Liu, C.H. Tang, Y. Chan, M. Elshazly, C.L. Lee, Y.C. Du, T.Y. Wu, F.R. Chang, Y.C. Wu, J. Agric. Food Chem. 64 (2016) 1540–1548.
[16] H.M. Xu, L. Pan, Y.L. Ren, Y.J. Yang, X.F. Huang, Z.D. Liu, Bioconjugate Chem. 22 (2011) 1386–1393.
[17] B. Zhou, Y. Wu, S. Dalal, M.B. Cassera, J.M. Yue, J. Nat. Prod. 79 (2016) 1952–1961.
[18] F.H. Fang, W.H. Li, Z.Z. Han, W.J. Huang, D.X. Li, S. Zhao, M.H. Tang, C.S. Yuan, J. Asian Nat. Prod. Res. 17 (2015) 1213–1219.
[19] C.S. Huang, S.H. Luo, Y.L. Li, C.H. Li, J. Hua, Y. Liu, S.X. Jing, Y. Wang, M.J. Yang, S.H. Li, Nat. Prod. Bioprospect. 4 (2014) 91–100.
[20] R.Y. Tian, Y. Lu, D.F. Chen, Chem. Biodivers. 13 (2016) 1404–1409.
[21] F. He, J.X. Pu, S.X. Huang, W.L. Xiao, L.B. Yang, X.N. Li, Y. Zhao, J. Ding, C.H. Xu, H.D. Sun, Helv. Chim. Acta 91 (2008) 2139–2147.
[22] A.S. Ng, Phytochemistry 29 (1990) 662–664.
[23] H.D. Flack, G. Bernardinelli, Acta Cryst. Sect. A 55 (1999) 908–991.
[24] R.W.W. Hooft, L.H. Straver, A.L. Spek, J. Appl. Crystallogr. 41 (2008) 96.